ELSEVIER

Progress in Biophysics & Molecular Biology 85 (2004) 279–299

Progress in Biophysics & Molecular Biology

www.elsevier.com/locate/pbiomolbio

Simulation of ATP metabolism in cardiac excitation–contraction coupling

Satoshi Matsuoka*, Nobuaki Sarai, Hikari Jo, Akinori Noma

Department of Physiology and Biophysics, Kyoto University Graduate School of Medicine, Yoshida-Konoe, Sakyo-Ku, Kyoto, 606-8501, Japan

Abstract

To obtain insights into the mechanisms underlying the membrane excitation and contraction of cardiac myocytes, we developed a computer model of excitation–contraction coupling (Kyoto model: Jpn. J. Physiol. 53 (2003) 105). This model was further expanded by incorporating pivotal reactions of ATP metabolism; the model of mitochondrial oxidative phosphorylation by Korzeniewski and Zoladz (Biophys. Chem. 92 (2001) 17). The ATP-dependence of contraction, and creatine kinase and adenylate kinase were also incorporated. After minor modifications, the steady-state condition was well established for all the variables, including the membrane potential, contraction, and the ion and metabolite concentrations in sarcoplasmic reticulum, mitochondria and cytoplasm. Concentrations of major metabolites were close to the experimental data. Responses of the new model to anoxia were similar to experimental results of the P-31 NMR study in whole heart. This model serves as a prototype for developing a more comprehensive model of excitation–contraction–metabolism coupling.

Keywords: Simulation; Heart; Metabolism; Excitation–contraction coupling

1. Introduction

Several computer models of membrane excitation have been developed for various types of cardiac ventricular myocyte (for examples, DiFrancesco and Noble, 1985; Luo and Rudy, 1991, 1994; Rice et al., 1999). These models describe detailed mechanisms of individual channels and transporters, and reconstruct well the characteristics of action potential and intracellular ion concentration changes. However, in these models, the contraction mechanism and ATP metabolism, which are essential for muscle contraction, were not included. Ch'en et al. (1998) first succeeded in incorporating both contraction mechanism (cross-bridge dynamics) and ATP

*Corresponding author. Tel.: +81-75-753-4357; fax: +81-75-753-4349.
E-mail address: matsuoka@card.med.kyoto-u.ac.jp (S. Matsuoka).

0079-6107/$ - see front matter
doi:10.1016/j.pbiomolbio.2004.01.006

metabolism into their ventricular cell model. In their model, cross-bridge formation was expressed in a simple algebraic equation, and some of the major mechanisms of ATP metabolism were incorporated, for example, creatine kinase, adenylate kinase and glycogen metabolism. Recently we published a computer model (Kyoto model) of the ventricular and sinoatrial node pacemaker cells (Matsuoka et al., 2003; Sarai et al., 2003). In our model, individual ion channels and transporters were described with a common set of equations for both the cell types, and the four-state kinetic model of contraction by Negroni and Lascano (1996) was incorporated. This model reconstructs well the experimental data of ventricular muscle contraction, including the intracellular Ca^{2+} dependence. ATP consumption by several ATPases was calculated, and ATP synthesis was modeled in a simplified equation.

To further approach the actual cardiac myocyte, we made improvements upon the Kyoto model by incorporating mitochondrial oxidative phosphorylation process, reactions of creatine kinase and adenylate kinase, and ATP dependence of contraction. We used a model of mitochondrial oxidative phosphorylation in the mammalian skeletal muscle developed by Korzeniewski and Zoladz (2001) after minor modifications. In this article, we briefly describe our current approach to simulate excitation–contraction–ATP metabolism coupling.

2. Methods

We modified the Kyoto model (Matsuoka et al., 2003) to simulate ATP metabolism related to the E–C coupling. Model equations and parameters used in this study are listed in Tables 1–13. The program was written by Delphi (Borland). The numeric data type of 'double precision' was used for all variables and the differential equations were integrated by using the fourth-order Runge–Kutta method. To shorten calculation time, the time interval (dt) was adaptively changed between 0.1 and 0.3 ms. A further decrease in dt did not significantly change the results, but calculation time increased.

Simulated membrane potential, half sarcomere length, intracellular Ca^{2+} transient, and major ionic currents and transporters are shown in Fig. 1. These results are essentially the same as those before the incorporation of the ATP metabolism (Matsuoka et al., 2003).

Fig. 2 illustrates an overview of ATP-related processes in this Kyoto model. As an ATP production system, mitochondrial oxidative phosphorylation, creatine kinase and adenylate kinase were incorporated. The ATP consumption by Na^+ pump, contraction (myosine ATPase) and sarcoplasmic reticulum Ca^{2+} pump (SERCA) were calculated (ATP consumption system). The two ATP-sensitive systems (L-type Ca^{2+} channel and ATP-sensitive K^+ channel) were incorporated. The diffusion and compartmentation of ATP were not taken into account for the sake of simplicity.

2.1. Modeling ATP production system: creatine kinase and adenylate kinase

We formulated the reaction of creatine kinase and adenylate kinase (Table 5). The apparent equilibrium constant of creatine kinase reaction was available from a literature (Herasymowych et al., 1978), but the forward and backward rate constants were not available. Since this reaction is known to be rapid, the forward and backward rate constants were empirically determined to be nearly instantaneous. Rate constant of adenylate kinase was obtained from a literature (Thuma et al., 1972).

Table 1
Abbreviations

Membrane excitation	
C_m	Membrane capacitance (pF)
CF_X	Constant field equation for ion X (mM)
E_x	Equilibrium potential for ion X (mV)
F	Faraday's constant, 96.4867 C mmol^{-1}
G_x	Conductance (pA/mV)
I_aX	Ion X component of current I_a (pA)
I_{bNSC}	Background non-selective cation current (pA)
I_{Cab}	Background Ca^{2+} current (pA)
I_{CaL}	L-type Ca^{2+} current (pA)
i_{CaL}	Single channel current of I_{CaL} (pA)
I_{CaT}	T-type Ca^{2+} current (pA)
I_{ext}	Current applied through the electrode (pA)
I_{ha}	Hyperpolarization-activated cation current (pA)
I_{K1}	Inward rectifier K^+ current (pA)
I_{KATP}	ATP-sensitive K^+ current (pA)
I_{Kpl}	Non-specific, voltage-dependent outward current (plateau current) (pA)
I_{Kr}	Delayed rectifier K^+ current, rapid component (pA)
I_{Ks}	Delayed rectifier K^+ current, slow component (pA)
I_l	Total of background current (time-independent) components (pA)
$I_{l(Ca)}$	Ca^{2+}-activated background cation current (pA)
I_{Na}	Na^+ current (pA)
I_{NaCa}	Na^+/Ca^{2+} exchange current (pA)
I_{NaK}	Na^+/K^+ pump current (pA)
$I_{net}X$	Whole cell current carried by ion X (pA)
I_{RyR}	Ca^{2+} release through the RyR channel in SR (pA)
$I_{SR}L$	Ca^{2+} leak from the SR (pA)
$I_{SR}U$	Ca^{2+} uptake in the SR (pA)
$I_{SR}T$	Ca^{2+} transfer from the SR uptake site to the release site (pA)
I_{to}	Transient outward current (pA)
I_{tot}	Total current of ion channels and ion exchangers (pA)
K_{mX}	Michaelis constant for ion X binding (mM)
N	Total number of channels
P_x	Convert factor (pA mM^{-1})
p(X)	Probability of state X in a multiple states gate
R	Gas constant, 8.3143 C mV K^{-1} mmol^{-1}
T	Absolute temperature K
V_i	Cell volume accessible for ion diffusion (μm^3)
V_m	Membrane potential (mV)
V_{mit}	Volume of mitochondria (μm^3)
V_{rel}	Volume of SR release site (μm^3)
V_{test}	Command potential in the voltage clamp (mV)
V_{up}	Volume of SR uptake site (μm^3)
y_n	Gating variable for two states gate ($0 \leq y_n \leq 1$)
z_X	Valence of ion X
[X]	Concentration of X (mM)
k, k_f, k_b $\alpha\beta\mu\lambda$	Rate constants (msec^{-1})

Table 1(*continued*)

Contraction	
ExternalForce	external force (= *ForceCB* + *ForceEcomp*)
ForceEcomp	Elastic component of force (arbitrary unit)
ForceCB	Cross-bridge force (arbitrary unit)
h	Cross-bridge elongation
hSML	Half sarcomere length (hSML = X + h)
T	thin filament site with free troponin C
TCa	thin filament site with troponin C bound to Ca
TCa*	thin filament site with troponin C bound to Ca and attached cross bridge(force generator)
T*	thin filament site with attached cross bridge and with free troponin C (force generator)
X	Length composed of half of the thick filament and the free portion of the thin filament)
Mitochondria and ATP metabolism	
a^{2+}	reduced cytochorome a_3 (a^{2+}) (mM)
a^{3+}	cytochrome a_3 (a^{3+}) (mM)
$A_{3/2}$	Ratio of oxidized a^{3+} to a^{2+}
$dATP\_AK$	ATP production rate by adenylate kinase (mM msec^{-1})
$dATP_{CaPump}$	Rate of ATP consumption by SERCA (mM msec^{-1})
$dATP\_CK$	ATP production rate by creatine kinase (mM msec^{-1})
$dATP_{Contraction}$	Rate of ATP consumption by contraction (mM msec^{-1})
$dATP_{INaK}$	Rate of ATP consumption by Na^+ pump (mM msec^{-1})
$dATP_{total,i}$	Rate of cytoplasmic ATP change (mM msec^{-1})
$dATP_{total,mit}$	Rate of mitochondria total ATP production (mM msec^{-1})
$dADP_{total,i}$	Rate of cytoplasmic ADP change (mM msec^{-1})
dc^{2+}_{mit}	Rate of reduced cytochorome c^{2+} (c^{2+}) production (mM msec^{-1})
dH_{mit}	Rate of mitochondria H^+ change (mM msec^{-1})
$dNADH_{mit}$	Rate of NADH production (mM msec^{-1})
$dPhosphoCreatine_i$	Rate of cytoplasmic phosphocreatine change (mM msec^{-1})
$dPI_{total,mit}$	Rate of mitochondria total PI production (mM msec^{-1})
$dUQH_{2mit}$	Rate of reduced ubiquinone (UQH_2) production (mM msec^{-1})
ΔG_{C1}	Thermodynamic span of complex I (mV)
ΔG_{C3}	Thermodynamic span of complex III (mV)
ΔG_{SN}	Thermodynamic span of ATP synthase (mV)
E_{ma}	cytochrome a_3 redox potential (mV)
E_{mc}	cytochrome c redox potential (mV)
E_{mN}	NAD redox potential (mV)
E_{mU}	ubiquinone redox potential (mV)
$r_{buffer,mit}$	buffering capacity for H^+ in mitochondria
R_{mc}	Ratio of mitochondria volume to cell volume
v_{DH}	Rate of substrate dehydrogenation in mitochondria (mM msec^{-1})
v_{C1}	Rate of Complex I (mM msec^{-1})
v_{C3}	Rate of Complex III (mM msec^{-1})
v_{C4}	Rate of Complex IV (mM msec^{-1})
v_{SN}	Rate of ATP synthase (mM msec^{-1})
v_{EX}	Rate of ATP/ADP exchanger (mM msec^{-1}):
v_{PI}	Rate of Phosphate carrier (mM msec^{-1}):
v_{LK}	Rate of Proton leak(mM msec^{-1}):

Table 2
Cell volume

	V_i (μm^3)	V_{rel} (μm^3)	V_{up} (μm^3)	C_m (pF)
Ventricular cell	$(100 \cdot 20 \cdot 8)/2$	$0.02 \cdot V_i$	$0.05 \cdot V_i$	132

Table 3
Ca^{2+}-binding proteins

	K_m (k_b/k_f) (mM)	k_f ($mM^{-1} ms^{-1}$)	k_b (ms^{-1})	Total concentration (μM)
TroponinC	7.70×10^{-4}	39	0.03	70
Calmodulin	2.38×10^{-3}	100	0.238	50
Calsequestrin	8.00×10^{-1}			10,000

Table 4
Calculation of the membrane potential and internal ion concentrations

Membrane potential

$$dV_m/dt = -(I_{tot} + I_{ext})/C_m$$
$$I_{tot} = I_{Na} + I_{CaL} + I_{CaT} + I_{K1} + I_{Kr} + I_{Ks} + I_{to} + I_l + I_{NaK} + I_{NaCa}$$
$$I_l = I_{bNSC} + I_{Cab} + I_{Kpl} + I_{l(Ca)} + I_{KATP}$$

Internal ion concentrations

$$d[Na]/dt = -I_{net}Na/F/V_I$$
$$d[K]/dt = -(I_{net}K + I_{ext})/F/V_I$$
$$d[Ca]/dt = -(I_{net}Ca - I_{RyR} + I_{SR}U - I_{SR}L)/z_{Ca}/F/V_i + (d[T] + d[T^*])/dt$$
$$I_{net}Na = I_{Na}Na + I_{CaL}Na + I_{to}Na + I_{Ks}Na + I_{bNSC}Na + I_{l(Ca)}Na + 3 \cdot I_{NaK} + 3 \cdot I_{NaCa}$$
$$I_{net}K = I_{K1} + I_{Kr} + I_{KATP} + I_{Na}K + I_{CaL}K + I_{to}K + I_{Ks}K + I_{bNSC}K + I_{l(Ca)}K + I_{Kpl} - 2 \cdot I_{NaK}$$
$$I_{net}Ca = I_{CaL}Ca + I_{CaT} + I_{Cab} - 2 \cdot I_{NaCa}$$

Constant field equation

$$CF_X = \frac{z_X \cdot F \cdot V_m}{R \cdot T} \frac{([X]_i - [X]_o \cdot \exp(\frac{-z_X \cdot F \cdot V_m}{R \cdot T}))}{(1 - \exp(\frac{-z_X \cdot F \cdot V_m}{R \cdot T}))}$$

We assumed that total concentrations of adenine, creatine and phosphate in cytoplasm are constant according to Allen and Orchard (1987).

2.2. Modeling ATP production system: mitochondrial oxidative phosphorylation

Korzeniewski's group has extensively studied the model of oxidative phosphorylation in mammalian skeletal muscle. We adopted their latest version (Korzeniewski and Zoladz, 2001) and incorporated it into the Kyoto model after minor modifications. Fig. 3 is a scheme of the mitochondrial oxidative phosphorylation model. Since the original model is based on

Table 5
Cytoplasmic energy balance

Creatine kinase

$$\text{Phosphocreatine} + \text{ADP}_{\text{total,i}} \underset{\leftarrow k_b}{\overset{\rightarrow k_f}{}} \text{ATP}_{\text{total,i}} + \text{Creatine}$$

$k_f = 16.\ 05\ (\text{ms}^{-1})$, $k_b = 9.67 \times 10^{-6}\ (\text{ms}^{-1})$

$\text{dATP\_CK} = k_f \times \text{ADP}_{\text{total,i}} \times \text{PhosphoCreatine-kb\_CK} \times \text{ATP}_{\text{total, i}} \times \text{Creatine}$

Adenylate kinase

$$\text{ADP}_{\text{free,i}} + \text{ADP}_{\text{Mg,i}} \underset{\leftarrow k_b}{\overset{\rightarrow k_f}{}} \text{ATP}_{\text{Mg,i}} + \text{AMP}_i$$

$k_f = 0.783\ (\text{ms}^{-1})$, $k_b = 0.683\ (\text{m s}^{-1})$

$\text{dATP\_AK} = k_f \times \text{ADP}_{\text{free, i}} \times \text{ADP}_{\text{Mg, i}} - k_b \times \text{ATP}_{\text{Mg, i}} \times \text{AMP}_i$

Total concentration of adenine, creatine and phosphate

$\text{A}_{\text{total,i}} = \text{ATP}_{\text{total, i}} + \text{ADP}_{\text{total, i}} + \text{AMP}_i = 7\ (\text{mM})$

$\text{C}_{\text{total}} = \text{Phosphocreatine}_i + \text{Creatine}_i = 25\ (\text{mM})$

$\text{P}_{\text{total}} = \text{Phosphocreatine}_i + \text{inorganic phosphate}_i + 3\text{ATP}_{\text{total,i}} + 2\text{ADP}_{\text{total,i}} + \text{AMP}_i = 46\ (\text{mM})$

$\text{ATP}_{\text{free, i}} = \text{ATP}_{\text{total, i}}/(1 + \text{Mg}_{\text{free, i}}/K_{\text{D, ATPi}})$, $K_{\text{D, ATPi}} = 0.024\ (\text{mM})$, $\text{Mg}_{\text{free, i}} = 4.0\ \text{mM}$

$\text{ATP}_{\text{Mg, i}} = \text{ATP}_{\text{total, i}} - \text{ATP}_{\text{free, i}}\ (\text{mM})$

$\text{ADP}_{\text{free, i}} = \text{ADP}_{\text{total, i}}/(1 + \text{Mg}_{\text{free, i}}/K_{\text{D, ADPi}})$, $K_{\text{D, ADPi}} = 0.347\ (\text{mM})$

$\text{ADP}_{\text{Mg, i}} = \text{ADP}_{\text{total, i}} - \text{ADP}_{\text{free, i}}\ (\text{mM})$

$\text{AMP}_i = \text{A}_{\text{total,i}} - \text{ATP}_{\text{total, i}} - \text{ADP}_{\text{total, i}}\ (\text{mM})$

$\text{inorganic phosphate}_i = \text{P}_{\text{total}} - (\text{PhosphoCreatine}_i + 3 \times \text{ATP}_{\text{total,i}} + 2 \times \text{ADP}_{\text{total,i}} + \text{AMP}_i + (3 \times \text{ATP}_{\text{total,mit}} + 2 \times \text{ADP}_{\text{total,mit}} + \text{PI}_{\text{total,mit}}) \times \text{R}_{\text{mc}})\ (\text{mM})$

$\text{dATP}_{\text{INaK}} = \frac{I_{\text{NaK}}}{F \cdot V_i}$

$\text{dATP}_{\text{CaPump}} = \frac{I_{\text{SR}}\, U}{4 \cdot F \cdot V_i}$

$\text{dATP}_{\text{Contraction}} = 0.4 \times \text{p(TCa}^*) \times \text{Troponin C}$

$\text{dATP}_{\text{total,i}} = v_{\text{EX}} + \text{dATP\_CK} + \text{dATP\_AK} - (\text{dATP}_{\text{INaK}} + \text{dATP}_{\text{CaPump}} + \text{dATP}_{\text{Contraction}})$

$\text{dADP}_{\text{total,i}} = -v_{\text{EX}} - \text{dATP\_CK} - 2 \times \text{dATP\_AK} + (\text{dATP}_{\text{INaK}} + \text{dATP}_{\text{CaPump}} + \text{dATP}_{\text{Contraction}})$

$\text{dPhosphoCreatine}_i = -\text{dATP\_CK}$

mitochondria of skeletal muscle, the volume ratio of mitochondria to the cell volume (6.7%) is smaller than that for cardiac myocytes. To simulate cardiac mitochondrial function, mitochondrial volume was increased to 23% (Schaper et al., 1985) and the ratio of the mitochondria volume to cell volume, R_{mc}, of 0.23 was used. All the rate constants of reactions were increased by 15 times to maintain steady state concentrations of cytoplasmic ATP and other metabolites. This model fitting may correspond to the fact that the cardiac mitochondria has larger cristae than those in the skeletal muscle.

2.3. *ATP consumption system: Na^+ pump and sarcoplasmic reticulum Ca^{2+} pump*

Numerical expressions of ATP dependence of the Na^+ pump and sarcoplasmic reticulum Ca^{2+} pump were the same as those described in our previous paper (Matsuoka et al., 2003). In the model of the two transporters, the rate constant k_1 was assumed to be ATP-dependent (Table 9).

Table 6
Inward currents

I_{Na}

$I_{Na} = I_{Na}\mathrm{Na} + I_{Na}K$
$I_{Na}\mathrm{Na} = P_{Na} \cdot CF_{Na} \cdot p(\mathrm{AP}) \cdot y$
$I_{Na}K = 0.1 \cdot p_{Na} \cdot CF_{K} \cdot p(AP) \cdot y$
$P_{Na} = 2860$

Voltage-dependent gate

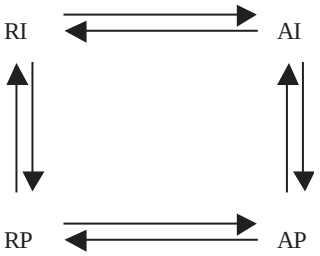

$k_{RP,AP} = 1/(0.1027 \cdot \exp(-V_m/8) + 0.25 \cdot \exp(-V_m/50))$
$k_{AP,RP} = 1/(26 \cdot \exp(V_m/17) + 0.02 \cdot \exp(V_m/800))$
$k_{RI,AI} = 1/(0.0001027 \cdot \exp(-V_m/8) + 5 \cdot \exp(-V_m/400))$
$k_{AI,RI} = 1/(1300 \cdot \exp(V_m/20) + 0.04 \cdot \exp(V_m/800))$
$k_{AP,AI} = 1/(0.8 \cdot \exp(-V_m/400))$
$k_{AI,\ AP} = 0.0000875$
$k_{RP,RI} = 0.01/(1 + k_{AI,AP} \cdot k_{AP,RP} \cdot k_{RI,AI}/k_{AP,AI}/k_{RP,AP}/k_{AI,RI})$
$k_{RI,RP} = 0.01 - k_{RP,RI}$

Ultra-slow gate

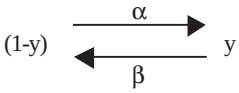

$\alpha_y = 1/(9,000,000,000 \cdot \exp(V_m/5) + 8000 \cdot \exp(V_m/100))$
$\beta_y = 1/(0.014 \cdot \exp(-V_m/5) + 4000 \cdot \exp(-V_m/100))$

I_{CaL}

$I_{CaL} = I_{CaL}\mathrm{Ca} + I_{CaL}K + I_{CaL}\mathrm{Na}$
$I_{CaL}\mathrm{Ca} = P_{CaL} \cdot \mathrm{CF_{Ca}} \cdot p(\mathrm{open_{CaL}})$
$I_{CaL}\mathrm{K} = 0.000365 \cdot P_{CaL} \cdot \mathrm{CF_K} \cdot p(\mathrm{open_{CaL}})$
$I_{CaL}\mathrm{Na} = 0.0000185 \cdot P_{CaL} \times \mathrm{CF_{Na}} \cdot p(\mathrm{open_{CaL}})$
$\mathrm{P_{CaL}} = 8712$
$p(\mathrm{open_{CaL}}) = p(\mathrm{AP}) \cdot (p(\mathrm{U}) + p(\mathrm{UCa})) \cdot y/(1 + (1.4/[ATP])^3)$

Voltage-dependent gate

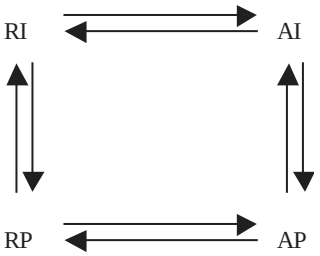

Table 6 (*continued*)

$k_{RP,AP} = 1/(0.27 \cdot \exp(-V_m/5.9) + 1.5 \cdot \exp(-V_m/65))$
$k_{AP,RP} = 1/(480 \cdot \exp(V_m/7) + 2.2 \cdot \exp(V_m/65))$
$k_{RI,AI} = 1/(0.0018 \cdot \exp(-V_m/7.4) + 2 \cdot \exp(-V_m/100))$
$k_{AI,RI} = 1/(2200,000 \cdot \exp(V_m/7.4) + 11 \cdot \exp(V_m/100))$
$k_{AP,AI} = 0.004, k_{AI,AP} = 0.001$
$k_{RP,RI} = 0.04/(1 + k_{AI,AP} \cdot k_{AP,RP} \cdot k_{RI,AI}/k_{AP,AI}/k_{RP,AP}/k_{AI,RI})$
$k_{RI,RP} = 0.04 - k_{RP,RI}$

Ca^{2+}-dependent gate

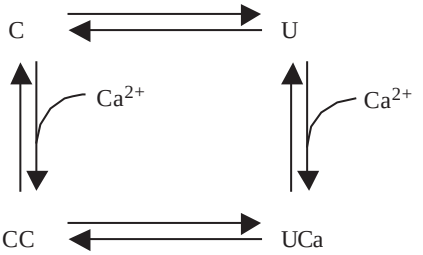

$k_{C,U} = 0.143, \quad k_{U,C} = 0.35$
$k_{CCa,UCa} = 0.0003, \quad k_{UCa,CCa} = 0.35$
$k_{C,CCa} = 6.954 \ (mM^{-1}ms^{-1}), \quad k_{CCa,C} = 0.0042$
$k_{U,UCa} = k_{C,CCa}, \ k_{UCa,U} = k_{CCa,C} \cdot k_{C,U} \cdot k_{UCa,CCa}/k_{U,C}/k_{CCa,UCa}$
$i_{CaL} = 0.0676 \cdot CF_{Ca}$
$[Ca^{2+}]_{cm} = [Ca^{2+}] - 0.3 \cdot i_{CaL}$
flux $(U \rightarrow UCa) = k_{U,UCa} \cdot p(U) \cdot ([Ca]_{cm} \cdot p(AP) + [Ca]_i \cdot (1 - p(AP)))$
flux $(C \rightarrow CCa) = k_{C,CCa} \cdot p(C) \cdot ([Ca]_{cm} \cdot p(AP))$

Ultra-slow gate

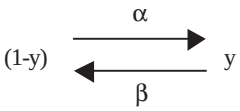

$\alpha_y = 1/(250,000 \cdot \exp(V_m/9) + 58 \cdot \exp(V_m/65))$
$\beta_y = 1/(1800 \cdot \exp(-V_m/14) + 66 \cdot \exp(-V_m/65))$

I_{CaT}

$I_{CaT} = 612 \cdot CF_{Ca} \cdot y_1 \cdot y_2$
$\alpha_{y1} = 1/(0.019 \cdot \exp(-V_m/5.6) + 0.82 \cdot \exp(-V_m/250))$
$\beta_{y1} = 1/(40 \cdot \exp(V_m/6.3) + 1.5 \cdot \exp(V_m/10,000))$
$\alpha_{y2} = 1/(62,000 \cdot \exp(V_m/10.1) + 30 \cdot \exp(V_m/3000))$
$\beta_{y2} = 1/(0.0006 \cdot \exp(-V_m/6.7) + 1.2 \cdot \exp(-V_m/25))$

The rate of ATP consumption by Na^+ pump was calculated based on its stoichiometry; $3Na^+$:$2K^+$:1ATP (Table 5). Data of ATP dependence of the Na^+ pump was taken from Collins et al. (1992, circles in Fig. 4A). The parameters were determined by fitting the data to our Na^+ pump model (solid curve in Fig. 4A). In this fitting, membrane potential (0 mV), extracellular

Table 7
Outward currents

I_{K1}

$$I_{K1} = G_{K1} \cdot (V_m - E_K) \cdot (f_O^4 + 4 \cdot 2/3 \cdot f_O^3 \cdot f_B + 6 \cdot 1/3 \cdot f_O^2 \cdot f_B^2) \cdot y$$
$$G_{K1} = 151.5 \cdot ([K]_o/5.4)^{0.4}$$
$$\alpha_y = 1/(8000 \cdot \exp((V_m - E_K - 97)/8.5) + 7 \cdot \exp((V_m - E_K - 97)/300))$$
$$\beta_y = 1/(0.00014 \cdot \exp(-(V_m - E_K - 97)/9.1) + 0.2 \cdot \exp(-(V_m - E_K - 97)/500))$$

$$O \underset{\lambda}{\overset{4\mu}{\rightleftarrows}} B_1 \underset{2\lambda}{\overset{3\mu}{\rightleftarrows}} B_2 \underset{3\lambda}{\overset{2\mu}{\rightleftarrows}} B_3 \underset{4\lambda}{\overset{\mu}{\rightleftarrows}} B_4$$

$$\mu = 0.75 \cdot \exp(0.035 \cdot (V_m - E_K - 10))/(1 + \exp(0.015 \cdot (V_m - E_K - 140)))$$
$$\lambda = 3 \cdot \exp(-0.048 \cdot (V_m - E_K - 10)) \cdot (1 + \exp(0.064 \cdot (V_m - E_K - 38)))$$
$$/(1 + \mathrm{Exp}(0.03 \cdot (V_m - E_K - 70)))$$
$$f_B = \mu/(\mu + \lambda)$$
$$f_O = \lambda/(\mu + \lambda)$$

I_{Kr}

$$I_{Kr} = G_{Kr} \cdot C_m \cdot (V_m - E_K) \cdot (0.6 \cdot y_1 + 0.4 \cdot y_2) \cdot y_3$$
$$G_{Kr} = 0.00864 \cdot ([K]_o/5.4)^{0.2}$$
$$\alpha_{y1} = 1/(20 \cdot \exp(-V_m/11.5) + 5 \cdot \exp(-V_m/300))$$
$$\beta_{y1} = 1/(160 \cdot \exp(V_m/28) + 200 \cdot \exp(V_m/1000)) + 1/(2500 \cdot \exp(V_m/20))$$
$$\alpha_{y2} = 1/(200 \cdot \exp(-V_m/13) + 20 \cdot \exp(-V_m/300))$$
$$\beta_{y2} = 1/(1600 \cdot \exp(V_m/28) + 2000 \cdot \exp(V_m/1000)) + 1/(10000 \cdot \exp(V_m/20))$$
$$\alpha_{y3} = 1/(10 \cdot \exp(V_m/17) + 2.5 \cdot \exp(V_m/300))$$
$$\beta_{y3} = 1/(0.35 \cdot \exp(-V_m/17) + 2 \cdot \exp(-V_m/150))$$

I_{Ks}

$$I_{Ks} = I_{Ks}K + I_{Ks}\mathrm{Na}$$
$$I_{Ks}\mathrm{K} = 5.04 \cdot \mathrm{CF_K} \cdot y_1^2 \cdot (0.9 \cdot y_2 + 0.1)$$
$$I_{Ks}\mathrm{Na} = 0.2016 \cdot \mathrm{CF_{Na}} \cdot y_1^2 \cdot (0.9 \cdot y_2 + 0.1)$$
$$\alpha_{y1} = 1/(85 \cdot \exp(-V_m/10.5) + 370 \cdot \exp(-V_m/62))$$
$$\beta_{y1} = 1/(1450 \cdot \exp(V_m/20) + 260 \cdot \exp(V_m/100))$$
$$\alpha_{y2} = 3.7 \cdot [Ca^{2+}]_i$$
$$\beta_{y2} = 0.004444$$

I_{to}

$$I_{to} = I_{to}K + I_{to}\mathrm{Na}$$
$$I_{to}\mathrm{K} = 0.033 \cdot \mathrm{CF_K} \cdot y_1^3 \cdot y_2$$
$$I_{to}\mathrm{Na} = 0.00297 \cdot \mathrm{CF_{Na}} \cdot y_1^3 \cdot y_2$$
$$\alpha_{y1} = 1/(11 \cdot \exp(-V_m/28) + 0.2 \cdot \exp(-V_m/400))$$
$$\beta_{y1} = 1/(4.4 \cdot \exp(V_m/16) + 0.2 \cdot \exp(V_m/500))$$
$$\alpha_{y2} = 0.0038 \cdot \exp(-(V_m + 13.5)/11.3)/(1 + 0.051335 \cdot \exp(-(V_m + 13.5)/11.3))$$
$$\beta_{y2} = 0.0038 \cdot \exp((V_m + 13.5)/11.3)/(1 + 0.067083 \cdot \exp((V_m + 13.5)/11.3))$$

Na^+ (0 mM) and K^+ (5 mM), and the intracellular Na^+ (100 mM) and K^+ (0 mM) were set equal to the original experiment. A similar approach was used for sarcoplasmic reticulum Ca^{2+} pump. The stoichiometry of the Ca^{2+} pump was assumed to be $2Ca^{2+}$:1ATP.

Table 8
Background currents

I_{bNSC}

$$I_{bNSC} = I_{bNSC}Na + I_{bNSC}K$$
$$I_{bNSC}Na = P_{bNSC} \cdot CF_{Na}$$
$$I_{bNSC}K = 0.4 \cdot P_{bNSC} \cdot CF_{K}$$
$$P_{bNSC} = 0.385$$

I_{Kpl}

$$I_{Kpl} = P_{Kpl} \cdot CF_{K} \cdot (V_m + 3)/(1 - \exp(-(V_m + 3)/13))$$
$$P_{Kpl} = 0.00011 \cdot ([K]_o/5.4)^{0.16}$$

$I_{l(Ca)}$

$$I_{l(Ca)} = I_{l(Ca)}K + I_{l(Ca)}Na$$
$$I_{l(Ca)}K = P_{l(Ca)} \cdot CF_{K} \cdot p(\text{open})$$
$$I_{l(Ca)}Na = P_{l(Ca)} \cdot CF_{Na} \cdot p(\text{open})$$
$$P_{l(Ca)} = 0.11$$
$$p(\text{open}) = \frac{1}{1+\left(\frac{0.0012}{[Ca^{2+}]_i}\right)^3}$$

I_{KATP}

$$I_{KATP} = N \cdot \gamma \cdot (V_m - E_K) \cdot p(\text{open})$$
$$N = 2333$$
$$\gamma = 0.0236 \cdot [K^+]_o^{0.24}$$
$$p(\text{open}) = \frac{0.8}{1+\left(\frac{[ATP]_i}{0.1}\right)^2}$$

I_{Cab}

$$I_{Cab} = P_{Cab} \cdot CF_{Ca}$$
$$P_{Cab} = 0.04$$

2.4. ATP consumption system: Contraction

We adopted a four-state model of contraction by Negroni and Lascano (1996) to simulate cardiac cell contraction (Table 11). Since ATP binding to a myosin head detaches the cross-bridge formation between myosin and actin, we assumed that all transition steps from cross-bridge-formed states ([T^*] and [TCa*]) to cross-bridge-released states ([T] and [TCa]) are ATP-dependent.

Data of ATP dependences of cardiac muscle were taken from Mekhfi and Ventura-Clapier (1988; skinned ventricular fibers). Parameters were determined by fitting the data (circles) to the modified Negroni and Lascano model (a solid curve) as shown at the left panel of Fig. 4B. Rate of ATP consumption by contraction ($dATP_{contraction}$) was assumed to be proportional to the concentration of [TCa*] state (Table 5).

Similarly, inhibition of contraction by inorganic phosphate (PI) was incorporated by modifying the α2 step. As shown at the right panel of Fig. 4B, the experimental data

Table 9
Exchanger and pumps

Na^+/Ca^{2+} *Exchange*

$$E_2Na \xleftrightarrow{KmNao} E_2 \xleftrightarrow{KmCao} E_2Ca \qquad (1-y)$$
$$k_1 \uparrow\downarrow k_2 \qquad\qquad k_3 \uparrow\downarrow k_4 \qquad\qquad \beta \uparrow\downarrow \alpha$$
$$E_1Na \xleftrightarrow{KmNai} E_1 \xleftrightarrow{KmCai} E_1Ca \qquad y$$

$K_{mNao} = 87.5$, $K_{mCao} = 1.38$, $K_{mNai} = 8.75$, $K_{mCai} = 0.00138$ (mM)
$k_1 = \exp(0.32 \cdot F \cdot V_m/R/T)$, $k_2 = \exp((0.32-1) \cdot F \cdot V_m/R/T)$, $k_3 = 1$, $k_4 = 1$
$p(E_1\mathrm{Na}) = 1/(1 + (K_{mNai}/[\mathrm{Na}]_i)^3 \cdot (1 + [\mathrm{Ca}]_i/K_{mCai}))$
$p(E_2\mathrm{Na}) = 1/(1 + (K_{mNao}/[\mathrm{Na}]_o)^3 \cdot (1 + [\mathrm{Ca}]_o/K_{mCao}))$
$p(E_1\mathrm{Ca}) = 1/(1 + (K_{mCai}/[\mathrm{Ca}]_i \cdot (1 + ([\mathrm{Na}]_i/K_{mNai})^3)))$
$p(E_2\mathrm{Ca}) = 1/(1 + (K_{mCao}/[\mathrm{Ca}]_o \cdot (1 + ([\mathrm{Na}]_o/K_{mNao})^3)))$

In the reduced two-state model,

$I_{NaCa} = 6.81 \cdot C_m \cdot (k_1 \cdot p(E_1\mathrm{Na}) \cdot y - k_2 \cdot p(E_2\mathrm{Na}) \cdot (1-y))$
$\alpha_y = k_2 \cdot p(E_2\mathrm{Na}) + k_4 \cdot p(E_2\mathrm{Ca})$
$\beta_y = k_1 \cdot p(E_1\mathrm{Na}) + k_3 \cdot p(E_1\mathrm{Ca})$

Na^+/K^+ *Pump*

$$E_2Na \xleftrightarrow{KmNao} E_2 \xleftrightarrow{KmKo} E_2K \qquad (1-y)$$
$$k_1 \uparrow\downarrow k_2 \qquad\qquad k_3 \uparrow\downarrow k_4 \qquad\qquad \beta \uparrow\downarrow \alpha$$
$$E_1Na \xleftrightarrow{KmNai} E_1 \xleftrightarrow{KmKi} E_1K \qquad y$$

$K_{mNao} = 69.8$, $K_{mKo} = 0.258$, $K_{mNai} = 4.05$, $K_{mKi} = 32.88$ (mM)
$k_1 = 0.37 \cdot (1/(1 + 0.094/[\mathrm{ATP}]_i))$, $k_2 = 0.04$, $k_3 = 0.01$, $k_4 = 0.165$
$p(E_1\mathrm{Na}) = 1/(1 + (K_{mNai}/[\mathrm{Na}]_i)^{1.06} \cdot (1 + ([\mathrm{K}]_i/K_{mKi})^{1.12}))$
$p(E_1\mathrm{K}) = 1/(1 + (K_{mKi}/[\mathrm{K}]_i)^{1.12} \cdot (1 + ([\mathrm{Na}]_i/K_{mNai})^{1.06}))$
$p(E_2\mathrm{Na}) = 1/(1 + (K_{mNao}/[\mathrm{Na}]_{eff})^{1.06} \cdot (1 + ([\mathrm{K}]_o/K_{mKo})^{1.12}))$
$p(E_2\mathrm{K}) = 1/(1 + (K_{mKo}/[\mathrm{K}]_o)^{1.12} \cdot (1 + ([\mathrm{Na}]_{eff}/K_{mNao})^{1.06}))$
$[\mathrm{Na}]_{eff} = [\mathrm{Na}]_o \cdot \exp(-0.82 \cdot F \cdot V_m/R/T)$

In the reduced two-state model

$I_{NaK} = 21 \cdot C_m \cdot (k_1 \cdot p(E_1\mathrm{Na}) \cdot y - k_2 \cdot p(E_2\mathrm{Na}) \cdot (1-y))$
$\alpha_y = k_2 \cdot p(E_2\mathrm{Na}) + k_4 \cdot p(E_2\mathrm{K})$
$\beta_y = k_1 \cdot p(E_1\mathrm{Na}) + k_3 \cdot p(E_1\mathrm{K})$

SR Ca^{2+} *Pump*

$$E_2Ca \xleftrightarrow{KmCao} E_2 \qquad 1-y$$
$$k_1 \uparrow\downarrow k_2 \qquad\qquad k_3 \uparrow\downarrow k_4 \qquad\qquad \beta \uparrow\downarrow \alpha$$
$$E_1Ca \xleftrightarrow{KmCai} E_1 \qquad y$$

$K_{mCao} = 0.0008$ (mM), $K_{mCai} = 0.08$ (mM)
$k_1 = 0.01$, $k_2 = 1$, $k_3 = \frac{1}{\frac{0.1}{1+[\mathrm{ATP}]_i}}$ $k_4 = 0.01$
$p(E_1\mathrm{Ca}) = 1/(1 + K_{mCai}/[\mathrm{Ca}^{2+}]_{up})$
$p(E_1) = 1 - p(E_1\mathrm{Ca})$
$p(E_2\mathrm{Ca}) = 1/(1 + K_{mCao}/[\mathrm{Ca}^{2+}]_i)$

Table 9 (*continued*)

$p(E_2) = 1 - p(E_2\mathrm{Ca})$

In the reduced two-state model

$I_{SR}U = I_{max} \cdot (k_2 \cdot p(E_2\mathrm{Ca}) \cdot (1-y) - k_1 \cdot p(E_1\mathrm{Ca}) \cdot y)$

$I_{max} = 162,500$

$\alpha_y = k_2 \cdot p(E_2\mathrm{Ca}) + k_4 \cdot p(E_2)$

$\beta_y = k_1 \cdot p(E_1\mathrm{Ca}) + k_3 \cdot p(E_1)$

Table 10
RyR and SR Ca^{2+} kinetics

RyR channel

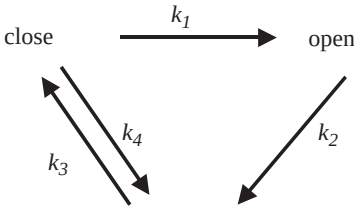

$k_1 = 280,000 \cdot [Ca^{2+}]_i^2 - 150 \cdot i_{CaL} \cdot p(\mathrm{open}_{CaL})$

$k_2 = 0.08/(1 + 0.36/[Ca^{2+}]_{rel})$

$k_3 = 0.000377 \cdot [Ca^{2+}]_{rel}^2, \quad k_4 = 0.000849$

$I_{RyR} = P_{RyR} \cdot ([Ca^{2+}]_{rel} - [Ca^{2+}]_i) \cdot p(\mathrm{open}_{RyR})$

$P_{RyR} = 62,000$

$I_{SR}T$

$I_{SR}T = P_{SR}T \cdot ([Ca]_{up} - [Ca]_{rel})$

$P_{SR}T = 386$

$I_{SR}L$

$I_{SR}L = P_{SR}L \cdot ([Ca]_{up} - [Ca]_i)$

$P_{SR}L = 459$

Ca^{2+} *concentrations in SR*

$d[Ca]_{rel}/dt = (I_{SR}T - I_{RyR})/z_{Ca}/F/V_{rel}$

$d[Ca]_{up}/dt = (I_{SR}U - I_{SR}T - I_{SR}L)/z_{Ca}/F/V_{up}$

(Mekhfi and Ventura-Clapier, 1988) of skinned ventricular fibers were well fitted by the modified Negroni and Lascano model.

2.5. ATP sensitive systems: L-type Ca^{2+} channel and ATP-sensitive K^+ channel

The ATP dependences of L-type Ca^{2+} channel ($p(\mathrm{open}_{CaL})$ in Table 6) and ATP-sensitive K^+ channel (p(open) in Table 8) were formulated as described in Matsuoka et al. (2003).

Table 11
Contraction

Contraction

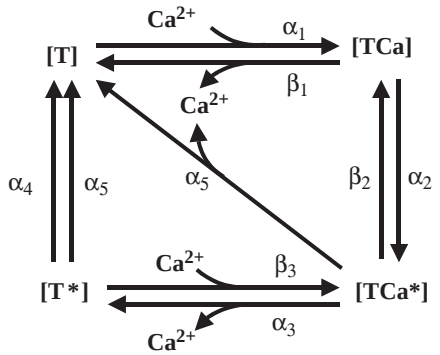

$\alpha_1 = 39\,(\mathrm{mM}\cdot\mathrm{ms}^{-1}),\quad \beta_1 = 0.03\,(\mathrm{ms}^{-1})$

$\alpha_2 = 0.0039 \times \left(0.54 \times \frac{KmPI_i}{KmPI_i + PI_i} + 0.46\right)\,(\mathrm{ms}^{-1})$

$\beta_2 = 0.0039 \cdot \frac{1}{1+\left(\frac{K_{\mathrm{mATP_i}}}{\mathrm{ATP_i}}\right)^3}\,(\mathrm{ms}^{-1})$

$\alpha_3 = 0.03\ \ (\mathrm{ms}^{-1}),\quad \beta_3 = 1560\ \ (\mathrm{mM\ ms}^{-1})$

$\alpha_4 = 0.12 \cdot \frac{1}{1+\left(\frac{K_{\mathrm{mATP_i}}}{\mathrm{ATP_i}}\right)^3}\ \ (\mathrm{ms}^{-1}),\quad \alpha_5 = 0.027 \cdot \frac{1}{1+\left(\frac{K_{\mathrm{mATP_i}}}{\mathrm{ATP_i}}\right)^3}\ \ (\mathrm{ms}^{-1})$

$K_{\mathrm{mPI_i}} = 1.83\ \ \mathrm{mM},\quad K_{\mathrm{mATP_i}} = 0.1\ \ \mathrm{mM}$

$\mathrm{d}X/\mathrm{d}t = -B \cdot (h - h_c),\quad B = 1.2\ \mathrm{ms}^{-1},\quad h_c = 0.005\ \mu\mathrm{m}$
$\mathrm{effectiveTCa} = \mathrm{e}^{-20\cdot(\mathrm{hSML}-1.17)^2}$
$Q_1 = \alpha_1 \cdot \mathrm{Ca}_i \cdot P(T) - \beta \cdot P(\mathrm{TCa})$
$Q_2 = \alpha_2 \cdot P(\mathrm{TCa}) \cdot \mathrm{effectiveTCa} - \beta_2 \cdot P(\mathrm{TCa}^*)$

$Q_3 = \alpha_3 \cdot P(\mathrm{TCa}^*) - \beta_3 \cdot \mathrm{Ca}_i \cdot P(T^*)$
$Q_4 = \alpha_4 \cdot P(T^*) + \alpha_5 \cdot (\mathrm{d}X/\mathrm{d}t)^2 \cdot P(T^*)$
$Q_5 = \alpha_5 \cdot (\mathrm{d}X/\mathrm{d}t)^2 \cdot P(\mathrm{TCa}^*)$
$\mathrm{d}P(\mathrm{TCa}) = Q_1 - Q_2$
$\mathrm{d}P(\mathrm{TCa}^*) = Q_2 - Q_3 - Q_5$
$\mathrm{d}P(T^*) = Q_3 - Q_4$
$P(T) = 1 - P(\mathrm{TCa}) - P(\mathrm{TCa}^*) - P(T^*)$
$\mathrm{ForceCB} = 1,800,000 \cdot \mathrm{TroponinC} \cdot ([\mathrm{TCa}^*] + [T^*]) \cdot (\mathrm{hSML} - X)$
$\mathrm{ForceEcomp} = 140,000 \cdot (0.97 - \mathrm{hSML})^5 + 200 \cdot (0.97 - \mathrm{hSML})$

Table 12
Mitochondria

$$v_{DH} = 15 \times 0.0004679 \frac{1}{\left(1+\frac{100}{NAD/NADH}\right)^{0.8}}$$

$$v_{C1} = 15 \times 0.0000039825 \cdot \Delta G_{C1}$$

$$v_{C3} = 15 \times 0.0000022735 \cdot \Delta G_{C3}$$

$$v_{C4} = 15 \times 0.06 \cdot a^{2+} \cdot c^{2+} \cdot \frac{1}{1+\frac{0.0008}{O_2}}$$

$$v_{SN} = 15 \times 0.00057193 \cdot \frac{\gamma-1}{\gamma+1}, \quad \gamma = 10^{\Delta G_{SN}/Zett}$$

$$v_{EX} = 15 \times 0.000909533 \cdot \left(\frac{ADP_{free,i}}{ADP_{free,i}+ATP_{free,i}\cdot 10^{-\psi_i/Zett}} - \frac{ADP_{free,mit}}{ADP_{free,mit}+ATP_{free,mit}\cdot 10^{-\psi_m/Zett}}\right)\left(\frac{1}{1+0.0035/ADP_{free,i}}\right).$$

$$v_{PI} = 15 \times 1.1570167 \cdot (PI_{ji} \cdot H_i - PI_{jmit} \cdot H_{mit})$$
$$PI_{ji} = PI_{total,i}/(1 + 10^{pH_i-6.8}), PI_{jmit} = PI_{total,mit}/(1 + 10^{pH_{mit}-6.8})$$
$$v_{LK} = 15 \times 0.0000000416667 \cdot (e^{0.038\cdot\Delta P} - 1)$$

Differential equations

$$dNADH_{mit} = (v_{DH} - v_{C1})/R_{mc}/5$$
$$dUQH2_{mit} = (v_{C1} - v_{C3})/R_{mc}$$
$$dc^{2+}_{mit} = (v_{C3} - 2 \cdot v_{C4}) \cdot 2/R_{mc}$$
$$dH_{mit} = -(2 \cdot (2 + 2 \cdot u) \cdot v_{C4} + (4 - 2 \cdot u) \cdot v_{C3} + 4 \cdot v_{C1} - 2.5 \cdot v_{SN} - u \cdot v_{EX} - (1 - u) \cdot v_{PI} - v_{LK})/R_{mc}/r_{buffer,mit}$$
$$dATP_{total,mit} = (v_{SN} - v_{EX})/R_{mc}$$
$$dPI_{total,mit} = (v_{PI} - v_{SN})/R_{mc}$$

Calculations

$$c^{3+} = c_t - c^{2+}, \quad c_t = 0.27 \ (mM)$$
$$UQ = U_t - UQH_2, \quad U_t = 1.35 \ (mM)$$
$$NAD = N_t - NADH, \quad N_t = 2.97 \ (mM)$$
$$ADP_{total,mit} = A_{total,mit} - ATP_{total,mit}, \quad A_{total,mit} = 16.26 \ (mM)$$
$$ATP_{free,mit} = ATP_{total,mit}/(1 + Mg_{free,mit}/0.017) \ (mM), \quad Mg_{free,mit} = 0.38 \ (mM)$$
$$ATP_{Mg,mit} = ATP_{total,mit} - ATP_{free,mit} \ (mM)$$
$$ADP_{free,mit} = ADP_{total,mit}/(1 + Mg_{free,mit}/0.282) \ (mM)$$
$$ADP_{Mg,mit} = ADP_{total,mit} - ADP_{free,mit} \ (mM)$$
$$H_{mit} = 10^{-pH_{mit}} \cdot 1000, \ (mM)$$
$$\Delta pH = Zett \cdot (pH_{mit} - pH_i), \quad pH_i = 7.0$$
$$\Delta p = 1/(1 - u) \cdot \Delta pH$$
$$\Delta\psi = -(\Delta p - \Delta pH) \ (mV)$$
$$\psi_{mit} = 0.65 \cdot \Delta\psi \ (mV), \quad \psi_i = -0.35 \cdot \Delta\psi \ (mV)$$
$$Zett = 2.303 \cdot 1000 \cdot R \cdot T/F$$
$$u = \Delta\psi/\Delta p (= 0.861)$$
$$r_{buffer,mit} = 0.022/c_{0,mit}, \quad c_{0,mit} = (10^{-pH_{mit}} - 10^{-pH_{mit}-0.001})/0.001$$
$$\Delta G_{SN} = 2.5 \cdot \Delta p - \Delta G_P$$
$$\Delta G_P = 31.9 \cdot 1000/F + Zett \cdot \log(1000 \cdot ATP_{total,m}/ADP_{total,m}/PI_{total,m})$$
$$\Delta G_{C1} = E_{mU} - E_{mN} - \Delta p \times 4/2$$

Table 12 (*continued*)

$$\Delta G_{C3} = E_{mc} - E_{mU} - \Delta p \times (4 - 2u)/2$$
$$E_{mN} = E_{mN0} + \mathrm{Zett}/2 \times \log\,(\mathrm{NAD^+/NADH}), \quad E_{mN0} = -320 \ \ (\mathrm{mV})$$
$$E_{mU} = E_{mU0} + \mathrm{Zett}/2 \times \log\,(\mathrm{UQ/UQH_2}), \quad E_{mU0} = 85 \ \ (\mathrm{mV})$$
$$E_{mc} = E_{mc0} + \mathrm{Zett} \times \log\,(c^{3+}/c^{2+}), \quad E_{mc0} = 250 \ \ (\mathrm{mV})$$
$$E_{ma} = E_{mc} + \Delta p \times (2 + 2u)/2$$
$$A_{3/2} = 10^{(E_{ma} - E_{ma0})/\mathrm{Zett}}, \quad E_{ma0} = 540 \ \ \mathrm{mV}$$
$$a^{2+} = a_t/(1 + A_{3/2}), \quad a^{3+} = a_t - a^{2+}, \quad a_t = 0.135 \ \ \mathrm{mM}$$

Table 13
Initial values

Parameters		Initial values	Parameters		Initial values
V_m		−85.766	$I_{SR}U$		
I_{Na}				y	0.4530
	RP	0.3553	Contraction		
	AP	1.746×10^{-5}		TCa	0.02497
	AI	0.4060		TCa*	0.001397
	y	0.5953		T^*	0.0002967
I_{CaL}				X	0.005011
	RP	0.9970		L	0.9647
	AP	1.574×10^{-6}	Cytosol		
	AI	0.0008623		$CMDN_{free}$	0.04962
	C	0.4298		$[K^+]_i$	141.9
	U	0.1744		$[Na^+]_i$	4.901
	UCa	0.00006016		$[Cai]_i$	18.25×10^{-6}
	y	0.9986		$ATP_{total,i}$	6.966
I_{CaT}				$ADP_{total,i}$	0.03361
	y_1	1.7468×10^{-5}		AMP_i	1.3737×10^{-5}
	y_2	0.8552		PI_i	2.5934
I_{K1}				Creatine	13.6433
	y	0.6081		PhosphoCreatine	11.3567
I_{Kr}				pHi	7.0 (fixed)
	y_1	0.001776	SR		
	y_2	0.2006		$CSQN_{free}$	2.6985
	y_3	0.9675		$Ca_{SR\ rel}$	9.4662
I_{Ks}				$Ca_{SR\ up}$	2.6106
	y_1	0.09331	Mitochondria		
	y_2	0.09577		c^{2+}	0.05107
I_{to}				O_2	0.24
	y_1	0.0008022		UQH2	1.0528
	y_2	0.9999		NADH	0.7135
RyR				pH_{mit}	7.4140
	Close	0.1939		PI_{mit}	8.5753
	Open	0.0003470		$ATP_{total,mit}$	7.0934
I_{NaCa}				$ADP_{total,mit}$	9.1671
	y	0.9892			
I_{NaK}					
	y	0.5897			

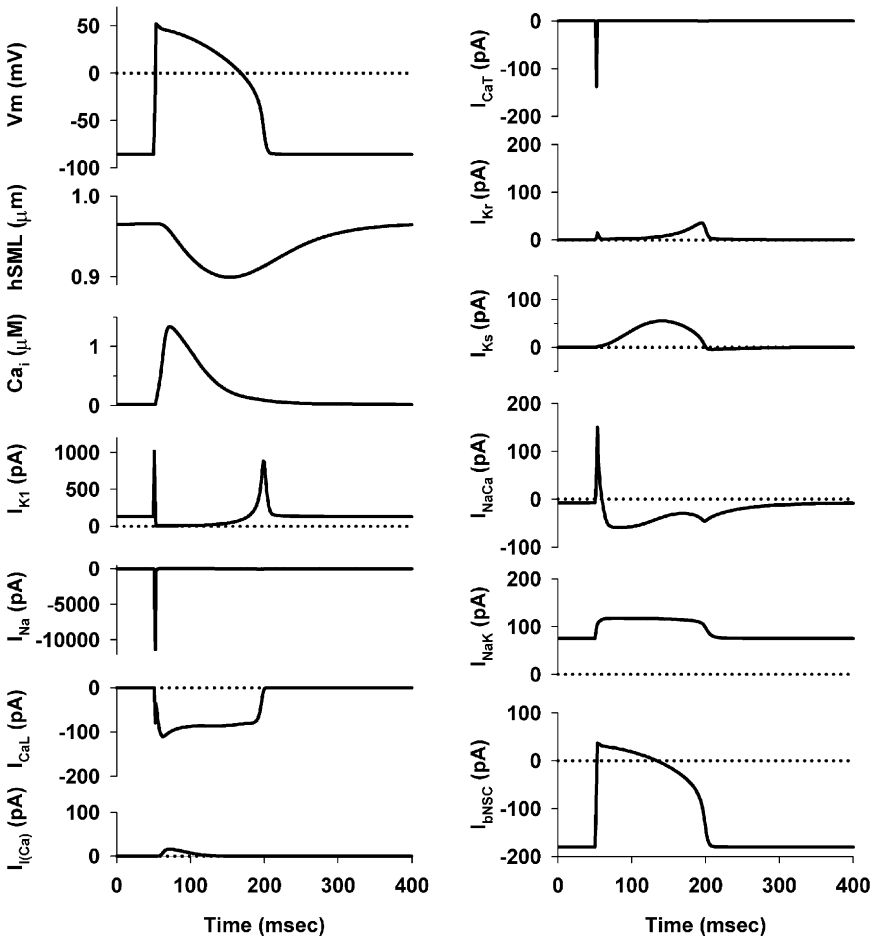

Fig. 1. Simulation of action potential, half sarcomere length, and major ionic currents and transporters. The model cell was stimulated at 2.5 Hz. The simulation results at steady state are shown.

3. Results

3.1. Steady-state concentrations of major metabolites

All the variables of this model, including the membrane potential, cytoplasmic ATP concentration, contraction, and ion concentrations in sarcoplasmic reticulum, mitochondria and cytoplasm, could reach steady state. Table 14 compares concentrations of major metabolites at the steady state. The myocyte was stimulated to induce action potential and contraction at 2.5 Hz. The steady-state concentrations of the metabolites are close to the experimental data (Kashiwaya et al., 1994; Dos Santos et al., 2000; Scott et al., 1994). These results suggest that our model is relevant for examining the response of cardiac myocyte to various interventions.

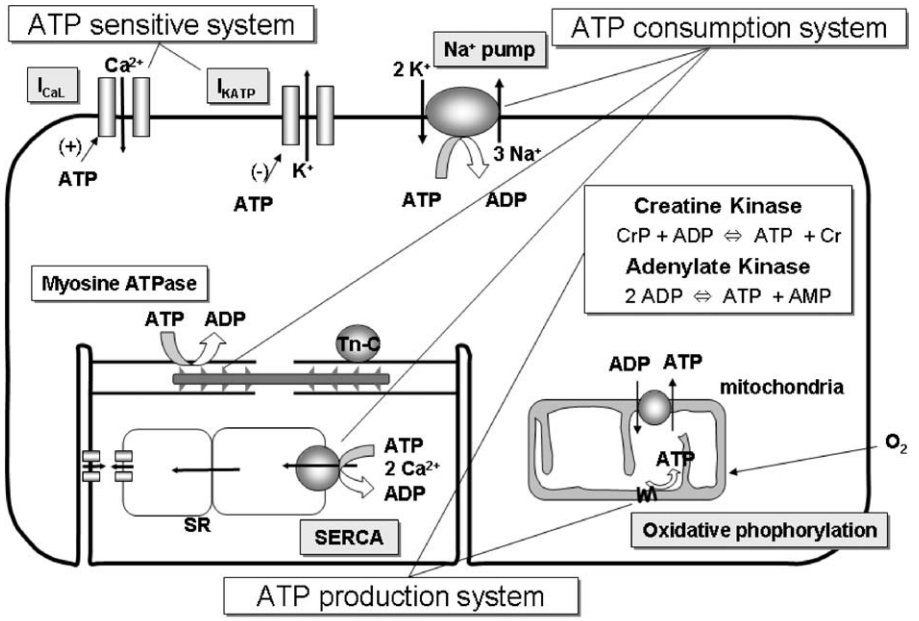

Fig. 2. Overview of ATP network in simulation. Abbreviations: sarcoplasmic reticulum (SR), sarcoplasmic reticulum Ca^{2+} pump (SERCA), and troponin C (Tn-C).

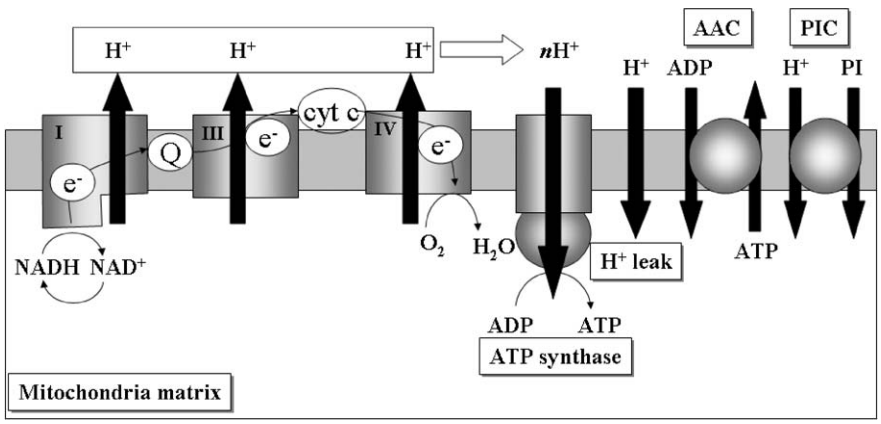

Fig. 3. Scheme of mitochondrial oxidative phosphorylation. This scheme illustrates a model of oxidative phosphorylation in mammalian skeletal muscle (Korzeniewski and Zoladz, 2001). Abbreviations: complex I (I), complex III (III), complex IV (IV), ubiquinone (Q), cytochrome *c* (cyt C), ATP/ADP exchanger (AAC), and proton–inorganic phosphate cotransporter (PIC).

3.2. *Fig. 6. Simulation of anoxia*

We tested the response of model to anoxia in Fig. 5. The myocyte was stimulated at 2.5 Hz, and the oxygen was completely depleted at time 0. The cessation of oxygen supply stopped the electron transport chain at complex IV, resulting in the depression of ATP synthesis via the decrease in the pH gradient across the inner membrane. However, as demonstrated in Fig. 5A, the intracellular

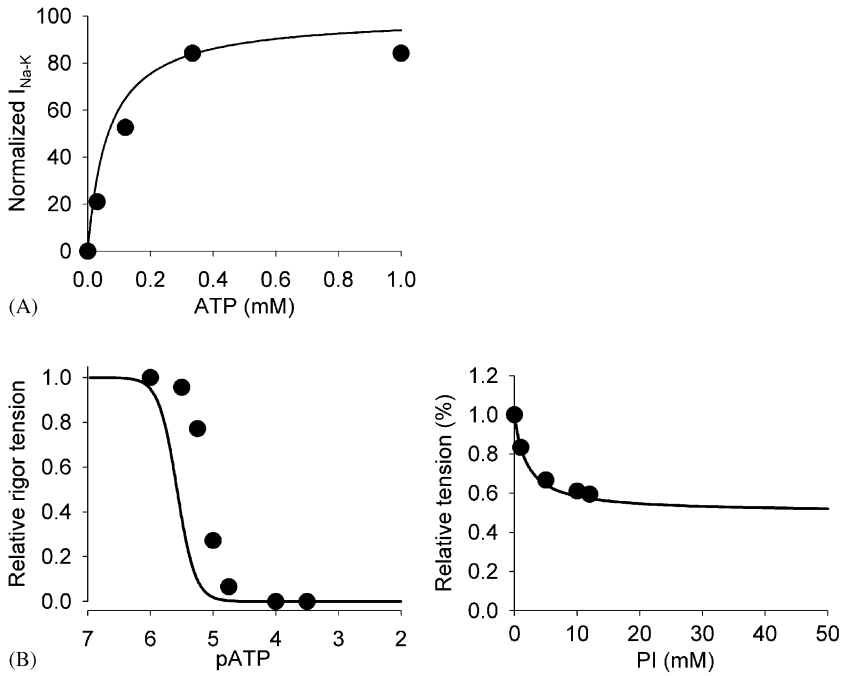

Fig. 4. Data fitting to the models of Na^+ pump and contraction. A. ATP dependence of Na^+ pump model. ATP dependence of the model (solid curve) and experimental data (circles, Collins et al., 1992) are plotted. B. ATP dependence of contraction (developed tension, right panel). Simulation conditions are $Ca_i^{2+} = 1$ nM and PI = 0 mM. Inorganic phosphate dependence of contraction (left panel). $Ca_i^{2+} = 1$ μM and ATP = 5 mM. Data (circles) are from Mekhfi and Ventura-Clapier (1988).

Table 14
Steady-state concentrations of major metabolites

	Rat heart Kashiwaya et al. (1994)	Rat heart Santos et al. (2000)	Glucose perfused rat heart Scott et al. (1994)	Kyoto model
PhosphoCreatine (mM)	7.1	16.7		11.4
Creatine (mM)	13.7	11.7		13.6
Inorganic Phosphate (mM)	4.88	3.7		2.6
ATP (mM)		11.8		6.97
ADP (mM)		0.055		0.0336
ATP/ADP	166	214.5		207
Mitochondria NADH/NAD			0.26	0.32

ATP concentration decreased only after a long delay. This preservation of intracellular ATP concentration at the early stage of anoxia is due to ATP production mainly by creatine kinase. It is evident that the ATP concentration decreases only after the phosphocreatine buffer is largely depleted. These results are in good agreement with P-31 NMR measurement of ischemic heart

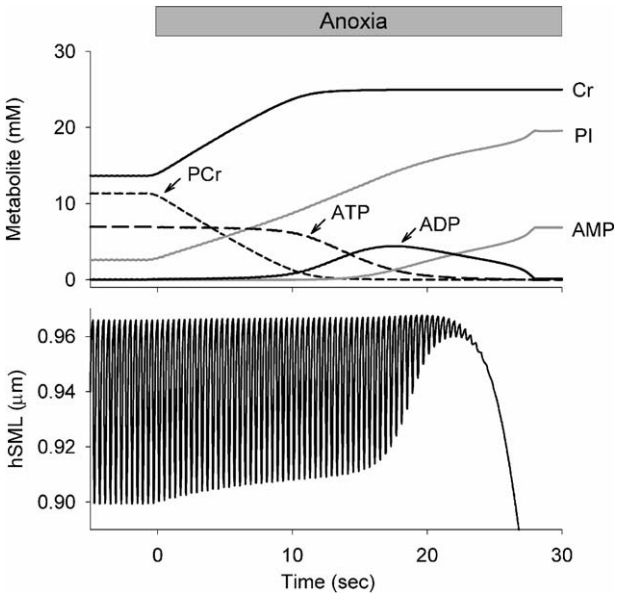

Fig. 5. Simulation of anoxia. Responses of creatine (Cr), phosphocreatine (PCr), ATP, ADP and AMP to anoxia are shown (upper panel). The lower panel shows half sarcomere length.

(Kay et al., 1997). It should be noted that the initial attenuation of contraction is mainly due to accumulation of inorganic phosphate in this model. The ATP-free rigor occurred about 20 s after the start of anoxia.

4. Discussion

In the previous studies (Matsuoka et al., 2003; Sarai et al., 2003), we combined, for the first time, our membrane excitation model with the contraction model (Negroni and Lascano, 1996) and demonstrated that the Kyoto model can simulate many of the important aspects of excitation–contraction coupling of ventricular myocytes. We described here further expansion of the Kyoto model by implementing the ATP metabolism. With regard to the ATP production, we modeled a minimum number of important factors of the ATP-related metabolisms, including mitochondrial oxidative phosphorylation, creatine kinase and adenylate kinase. In consequence, the pattern of changes in the ATP-related substances during anoxia (Fig. 5) is consistent with P-31 NMR measurement of ischemic heart (Kay et al., 1997). The model demonstrated that the initial attenuation of developed tension is mainly due to the increase in inorganic phosphate. The time course of changes during the anoxic intervention is much faster in our simulation than that in the experimental data by Kay et al. (1997). This is probably because the perfusate could not be rapidly changed in the experiment and the removal of oxygen from the whole heart could not be perfect, while in the simulation the oxygen concentration was changed to zero instantaneously. In fact, the response of dissociated cardiac myocyte to anoxia was quite quick when the anoxic perfusion was performed using a special experimental setup (Benndorf et al., 1992).

The present model can well explain the respiratory control theory (Chance and Williams, 1956; Harris and Das, 1991), which asserts that the availability of ADP to ATP synthesis is the limiting factor for mitochondrial ATP production. In the present Kyoto model, mitochondria NADH decreases, if cell workload is increased by increasing the cell pacing rate (result not shown). This is consistent with the respiratory control theory. However, in our preliminary measurement of NADH autofluorescence of single guinea-pig ventricular cells, NADH fluorescence first decreased and then increased as observed in rat trabeculae (Brandes and Bers, 2002). The discrepancy between our simulation and the experimental data may suggest the existence of other mechanisms that regulate mitochondria NADH production. Recently, it was reported that inorganic phosphate (Bose et al., 2003) and Ca^{2+} (Brandes and Bers, 2002) control the mitochondrial ATP production. This working hypothesis of additional regulating mechanisms provided from the Kyoto model must be studied further by experiments and also by computer simulations.

Some of the modules in the Kyoto model should be further improved in the future. In the Korzeniewski model (Korzeniewski and Zoladz, 2001), NADH production by the TCA cycle is expressed by a simple equation. The whole TCA cycle should be substituted for the simple equation. Recently Cortassa et al. (2003) published a mitochondria model that includes the whole TCA cycle, mitochondria Ca^{2+} regulation and simplified oxidative phosphorylation. However, this model is not yet incorporated into a cardiac excitation–contraction model. Secondly, the glycolysis pathway and also fatty acid pathway should be incorporated to make the model cell dependent on extracellular nutrition. Finally, it should be important to model the intracellular pH regulation, because intracellular pH changes during ischemia or anoxia is associated with many metabolic reactions. The present Kyoto model will serve as a prototype for developing a more comprehensive model of excitation–contraction–metabolism coupling.

Acknowledgements

This study was supported by the Program for Promotion of Fundamental Studies in Health Sciences of the Organization for Pharmaceutical Safety and Research, a Grant-in-Aid for Scientific Research, and a Leading Project for Biosimulation from the Ministry of Education, Culture, Sports, Science and Technology (to S.M., N.S. and A.N).

References

Allen, D.G., Orchard, C.H., 1987. Myocardial contractile function during ischemia and hypoxia. Circ. Res. 60, 153–168.

Benndorf, K., Bollmann, G., Friedrich, M., Hirche, H., 1992. Anoxia induces time-independent K^+ current through K_{ATP} channels in isolated heart cells of the guinea-pig. J. Physiol. 454, 339–357.

Bose, S., French, S., Evans, F.J., Joubert, F., Balaban, R.S., 2003. Metabolic network control of oxidative phosphorylation: Multiple roles of inorganic phosphate. J. Biol. Chem. 278, 39155–39165.

Brandes, R., Bers, D.M., 2002. Simultaneous measurements of mitochondrial NADH and Ca^{2+} during increased work in intact rat heart trabeculae. Biophys. J. 83, 587–604.

Chance, B., Williams, G.R., 1956. The respiratory chain and oxidative phosphorylation. Adv. Enzymol. 17, 65–134.

Ch'en, F.F., Vaughan-Jones, R.D., Clarke, K., Noble, D., 1998. Modelling myocardial ischaemia and reperfusion. Prog. Biophys. Mol. Biol. 69, 515–538.

Collins, A., Somlyo, A.V., Hilgemann, D.W., 1992. The giant cardiac membrane patch method: stimulation of outward Na^+–Ca^{2+} exchange current by MgATP. J. Physiol. 454, 27–57.

Cortassa, S., Aon, M.A., Marban, E., Winslow, R.L., O'Rourke, B., 2003. An integrated model of cardiac mitochondrial energy metabolism and calcium dynamics. Biophys J. 84, 2734–2755.

DiFrancesco, D., Noble, D., 1985. A model of cardiac electrical activity incorporating ionic pumps and concentration changes. Philos. Trans. R. Soc. London B: Biol. Sci. 307, 353–398.

Dos Santos, P., Aliev, M.K., Diolez, P., Duclos, F., Besse, P., Bonoron-Adele, S., Sikk, P., Canioni, P., Saks, V.A., 2000. Metabolic control of contractile performance in isolated perfused rat heart. Analysis of experimental data by reaction: diffusion mathematical model. J. Mol. Cell. Cardiol. 32, 1703–1734.

Harris, D.A., Das, A.M., 1991. Control of mitochondrial ATP synthesis in the heart. Biochem. J. 280, 561–573.

Herasymowych, O.S., Mani, R.S., Kay, C.M., 1978. Isolation, purification and characterization of creatine kinase from bovine cardiac muscle. Biochim. Biophys. Acta. 534, 38–47.

Kashiwaya, Y., Sato, K., Tsuchiya, N., Thomas, S., Fell, D.A., Veech, R.L., Passonneau, J.V., 1994. Control of glucose utilization in working perfused rat heart. J. Biol. Chem. 269, 25502–25514.

Kay, L., Saks, V.A., Rossi, A., 1997. Early alteration of the control of mitochondrial function in myocardial ischemia. J. Mol. Cell. Cardiol. 29, 3399–33411.

Korzeniewski, B., Zoladz, J.A., 2001. A model of oxidative phosphorylation in mammalian skeletal muscle. Biophys. Chem. 92, 17–34.

Luo, C.H., Rudy, Y., 1991. A model of the ventricular cardiac action potential. Depolarization, repolarization, and their interaction. Circ. Res. 68, 1501–1526.

Luo, C.H., Rudy, Y., 1994. A dynamic model of the cardiac ventricular action potential. I. Simulations of ionic currents and concentration changes. Circ. Res. 74, 1071–1096.

Matsuoka, S., Sarai, N., Kuratomi, S., Ono, K., Noma, A., 2003. Role of individual ionic current systems in ventricular cells hypothesized by a model study. Jpn. J. Physiol. 53, 105–123.

Mekhfi, H., Ventura-Clapier, R., 1988. Dependence upon high-energy phosphates of the effects of inorganic phosphate on contractile properties in chemically skinned rat cardiac fibres. Pflugers Arch. 411, 378–385.

Negroni, J.A., Lascano, E.C., 1996. A cardiac muscle model relating sarcomere dynamics to calcium kinetics. J. Mol. Cell. Cardiol. 28, 915–929.

Rice, J.J., Winslow, R.L., Hunter, W.C., 1999. Comparison of putative cooperative mechanisms in cardiac muscle: length dependence and dynamic responses. Am. J. Physiol. 276, H1734–H1754.

Sarai, N., Matsuoka, S., Kuratomi, S., Ono, K., Noma, A., 2003. Role of individual ionic current systems in the SA node hypothesized by a model study. Jpn. J. Physiol. 53, 125–134.

Schaper, J., Meiser, E., Stammler, G., 1985. Ultrastructural morphometric analysis of myocardium from dogs, rats, hamsters, mice, and from human hearts. Circ. Res. 56, 377–391.

Scott, D.A., Grotyohann, L.W., Cheung, J.Y., Scaduto Jr., R.C., 1994. Ratiometric methodology for NAD(P)H measurement in the perfused rat heart using surface fluorescence. Am. J. Physiol. 267, H636–H644.

Thuma, E., Schirmer, R.H., Schirmer, I., 1972. Preparation and characterization of a crystalline human atp: amp phosphotransferase. Biochim. Biophys. Acta. 268, 81–91.